Base Pair Mismatches and Carcinogen-Modified Bases in DNA: An NMR Study of A·C and A·O⁴meT Pairing in Dodecanucleotide Duplexes†

Matthew W. Kalnik,‡ Michael Kouchakdjian,‡ Benjamin F. L. Li,§,‖ Peter F. Swann,§ and Dinshaw J. Patel*,‡

Department of Biochemistry and Molecular Biophysics, College of Physicians and Surgeons, Columbia University, New York, New York 10032, and Courtauld Institute of Biochemistry, Middlesex Hospital Medical School, London, England W1P 7PN

Received June 23, 1987; Revised Manuscript Received September 8, 1987

ABSTRACT: Structural features of A·C mismatches and A·O⁴meT pairs in the interior of oligodeoxynucleotide duplexes have been investigated by high-resolution two-dimensional proton NMR spectroscopy on the self-complementary d(C-G-C-*A*-A-G-C-T-*C*-G-C-G) duplex (designated A·C 12-mer) and the self-complementary d(C-G-C-*A*-A-G-C-T-*O⁴meT*-G-C-G) duplex (designated A·O⁴meT 12-mer) containing A·C and A·O⁴meT pairs at identical positions four base pairs in from either end of the duplex. Proton NMR shows that there are similar pH-dependent changes in the structure in the A·C 12-mer and A·O⁴meT 12-mer duplexes. Our studies have focused on the low-pH (pH 5.5) conformation where high-quality two-dimensional NOESY data sets were collected from the exchangeable and nonexchangeable protons in these duplexes. The spectral parameters for the A·C 12-mer and the A·O⁴meT 12-mer duplexes were very similar, indicating that they must have similar structures at this pH in aqueous solution. Both structures are right-handed double helices with all the bases adopting the normal anti configuration about the glycosidic bond. The same atoms are involved in hydrogen-bond pairing for the A·C mismatch and the A·O⁴meT pair, and these pairs have a similar spatial relationship to flanking base pairs. X-ray crystallography [Hunter, W. N., Brown, T., Anand, N. N., & Kennard, O. (1986) *Nature (London) 320*, 552-555] recently confirmed the wobble pairing structure for the A·C mismatch, which had previously been suggested from NMR studies on solutions of oligonucleotide duplexes [Patel, D. J., Kozlowski, S. A., Ikuta, S., & Itakura, K. (1984) *Biochemistry 23*, 3218-3226] and from theoretical calculations [Keepers, J. W., Schmidt, P., James, T. L., & Kollman, P. A. (1984) *Biopolymers 23*, 2901-2929]. The comparative NMR study on the A·C 12-mer and A·O⁴meT 12-mer duplexes demonstrates similar wobble pairing for the A·O⁴meT lesion. We can monitor the amino protons of A in the A·C mismatch and the A·O⁴meT pair in the low-pH spectra (pH 5.5-6.0), providing additional markers at the modification sites. Further, the distance-dependent NOE measurements establish that the OCH_3 group of O⁴meT adopts a syn orientation with respect to N3 of the base and is directed toward the A on the partner strand in the A·O⁴meT pair. The lateral displacement of the bases in the wobble pairing allows the OCH_3 group in the syn orientation to be accommodated in the helix.

The alkylation of the 6-O of guanosine and the 4-O of thymidine in DNA is believed to play a critical role in the mutagenic and carcinogenic action of *N*-nitroso compounds (Pegg, 1977; Singer & Grunberger, 1983). Because the presence of *O⁴*-methylthymidine residues in DNA leads to mutation, in particular A·T → G·C transitions (Preston et al., 1986), and the residue is also recognized by DNA repair enzymes, there is interest in its base pairing properties and in possible structural changes in DNA. The base pairing of O⁴meT and associated perturbations in DNA structure have not been previously studied at the intact duplex level. We have therefore undertaken a research program aimed at studying the structure and dynamics of A·O⁴meT and G·O⁴meT pairs in the interior of oligonucleotide duplexes. This paper focuses on the A·O⁴meT pair while the following paper (Kalnik et al., 1988) focuses on the G·O⁴meT pair.

The C and O⁴meT bases differ only in the 4-position of the pyrimidine ring where the 4-NH_2 group in C is replaced by the 4-OCH_3 group in O⁴meT. We reasoned that a comparative study of the A·C base pair mismatch with the A·O⁴meT pair in otherwise identical oligonucleotide duplexes would be of great interest. The purine·pyrimidine A·C mismatch has been previously investigated at the dodecanucleotide level by one-dimensional NMR in solution (Patel et al., 1984a,b), by theoretical computations (Keepers et al., 1984), and by single-crystal X-ray studies in the solid state (Hunter et al., 1986). The NMR studies on pairing at the A·C mismatch site are limited by the fact that neither A nor C carries an imino proton, precluding unambiguous alignment of the bases. Wobble pairing was proposed for the A·C mismatch site on the basis of an analysis of one-dimensional NMR chemical shift and NOE studies (Patel et al., 1984a,b) and theoretical computations guided by the NMR results (Keepers et al., 1984). In this model, the A·C mismatch was stabilized by one hydrogen bond involving the cytidine N3 and the adenosine 6-amino proton. This pairing has now been confirmed by the single-crystal X-ray structure of the A·C mismatch in a dodecanucleotide (Hunter et al., 1986). In addition, these authors suggested that the A·C mismatch pair is further stabilized by a second hydrogen bond involving a protonated adenosine N1 nitrogen paired to the cytidine carbonyl group on the basis of the observed short nitrogen-carbon distance

† The research was supported from Start-Up Funds provided by Columbia University, by NIH Grant CA-46533 to D.J.P., and by grants from the Cancer Research Campaign and the Medical Research Council to P.F.S. The NMR spectrometers were purchased from funds donated from the Robert Woods Johnson Jr. Trust and Matheson Trust toward setting up an NMR Center in the Basic Medical Sciences at Columbia University.

‡ Columbia University.

§ Middlesex Hospital Medical School.

‖ Present address: Institute of Molecular and Cellular Biology, National University of Singapore, Kent Ridge, Singapore 0511.

0006-2960/88/0427-0100$01.50/0

in the crystal. The question of a second hydrogen bond involving a protonated adenosine ring at neutral pH in the A·C mismatch in solution remains to be established.

Experimental Procedures

The numbering system of the d(C-G-C-*A*-A-G-C-T-*C*-G-C-G) duplex (designated A·C 12-mer, I) and the d(C-G-C-*A*-A-G-C-T-*O⁴meT*-G-C-G) duplex (designated A·O⁴meT 12-mer, II) follow standard conventions. We have determined

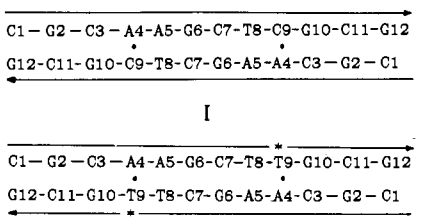

that incorporation of the modifications four base pairs in from either end of the duplex results in a conformational equilibrium between the fully paired duplex and a second minor form (probably a hairpin) of these dodecanucleotides. Our NMR studies are undertaken in 1.1 M NaCl, which shifts the equilibrium predominantly toward the fully paired duplex.

Sample Preparation. The A·C 12-mer and A·O⁴meT 12-mer were synthesized in milligram quantities by the solution-phase phosphotriester approach. The synthesis, purification, and characterization of the A·O⁴meT 12-mer duplex has been reported recently (Li et al., 1987). The NMR spectra were recorded in aqueous-solution buffer containing 1.1 M NaCl, 10 mM phosphate, and 1 mM ethylenediaminetetraacetic acid (EDTA) (henceforth designated high-salt buffer). The A·C 12-mer sample was prepared to a concentration of 400 A_{260} units in 0.4 mL of buffer while the concentration of the A·O⁴meT 12-mer sample was 330 A_{260} units in 0.35 mL. The pH values quoted in D_2O solution are uncorrected pH meter readings.

NMR Experiments. Proton NMR spectra were recorded at 500 MHz on a Bruker AM 500 spectrometer. Two-dimensional magnitude NOESY spectra (mixing time 120 ms) were recorded in H_2O solution with a 1-1 pulse for excitation, mixing, and detection. The carrier frequency was shifted 6000 Hz downfield from the H_2O resonance and the 1-1 delay optimized for H_2O suppression. The time domain data sets consisted of 2048 complex data points over a sweep width of 15 000 Hz in the t_2 dimension. The repetition delay was 1.0 s, and 256 scans were collected for each t_1 increment. The free induction decays were apodized with an unshifted sine bell function zeroed at the 1024th point in the t_2 dimension and the 512th point in the t_1 dimension and Fourier transformed in both dimensions.

Two-dimensional phase-sensitive NOESY spectra (mixing time 250 ms) were recorded in D_2O solution with the carrier frequency positioned on the residual HOD resonance. The decoupling channel was used to suppress the residual HOD resonance. The time domain data sets were accumulated over a sweep width of 5000 Hz with 1024 complex data points in the t_2 dimension and 256 complex data points in the t_1 dimension. The repetition delay was 1.5 s, and 32 scans were collected for each t_1 increment. The free induction decays were apodized with a 30°-shifted sine bell function zeroed at the 1024th point in the t_2 dimension and at the 256th point in the t_1 dimension and Fourier transformed in both dimensions.

The two-dimensional data sets were processed with FTNMR software (D. Hare, unpublished programs) on VAX 11-780 and micro VAX-II computers. The two-dimensional contour plots were processed with the t_1 noise reduction routine of either Klevitt (1985) or Otting et al. (1986) and symmetrized prior to plotting on either Zeta 822 or HP 7475A plotters.

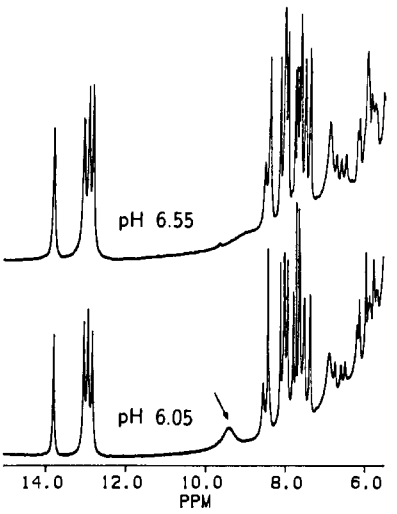

FIGURE 1: The 500-MHz proton NMR spectra (6–15 ppm) of the A·C 12-mer duplex in 1.1 M NaCl, 10 mM phosphate, and H_2O, 25 °C, at pH 6.55 and pH 6.05.

Results

The NMR data for the A·C 12-mer duplex (I) are presented first and are followed by the corresponding NMR data for the A·O⁴meT 12-mer duplex (II).

A·C 12-mer

Exchangeable Proton Spectra. The one-dimensional exchangeable proton spectra (6.0–15.0 ppm) of the A·C 12-mer in high-salt H_2O buffer, at pH 6.05 and 6.55, 25 °C, are plotted in Figure 1. Four imino proton resonances are detected between 12.5 and 14.0 ppm and correspond to the imino protons of the three nonterminal G·C base pairs and the one A·T base pair in the A·C 12-mer duplex (I). The imino proton of the terminal G·C base pair has broadened out due to fraying at the ends of the helix at this temperature. We observe an additional exchangeable resonance at 9.38 ppm in the pH 6.05 spectrum, which is very broad in the pH 6.55 spectrum of the A·C 12-mer duplex at 25 °C (Figure 1).

The resonances between 12.5 and 14.0 ppm in the A·C 12-mer duplex have been assigned to specific imino protons in the sequence by recording a magnitude NOESY spectrum (120-ms mixing time) in high-salt H_2O buffer, pH 6.55 at 15 °C. The imino proton region extending from 12.4 to 14.0 ppm is plotted in Figure 2A while the region linking the imino protons (12.4–14.0 ppm) with the amino and nonexchangeable base protons (7.4–8.8 ppm) is plotted in Figure 2B. The furthest downfield imino proton at 13.74 ppm exhibits an NOE to an adenosine H2 proton at 7.68 ppm (cross-peak C, Figure 2B), and these protons are assigned to the A5·T8 base pair. The three remaining guanosine imino protons exhibit NOEs within and between adjacent base pairs. The highest field guanosine imino proton at 12.75 ppm exhibits NOEs to the 7.93 ppm hydrogen-bonded cytidine amino proton (cross-peak H, Figure 2B) within the G·C base pair and to the thymidine imino proton (cross peak A, Figure 2A) and adenosine H2 proton (cross-peak D, Figure 2B) of the adjacent A5·T8 base pair. This permits assignment of the guanosine imino and cytidine amino protons to the G6·C7 base pair, which is adjacent to the A5·T8 base pair. The 12.85 ppm guanosine imino proton exhibits NOEs to the 8.49 ppm hydrogen-bonded cy-

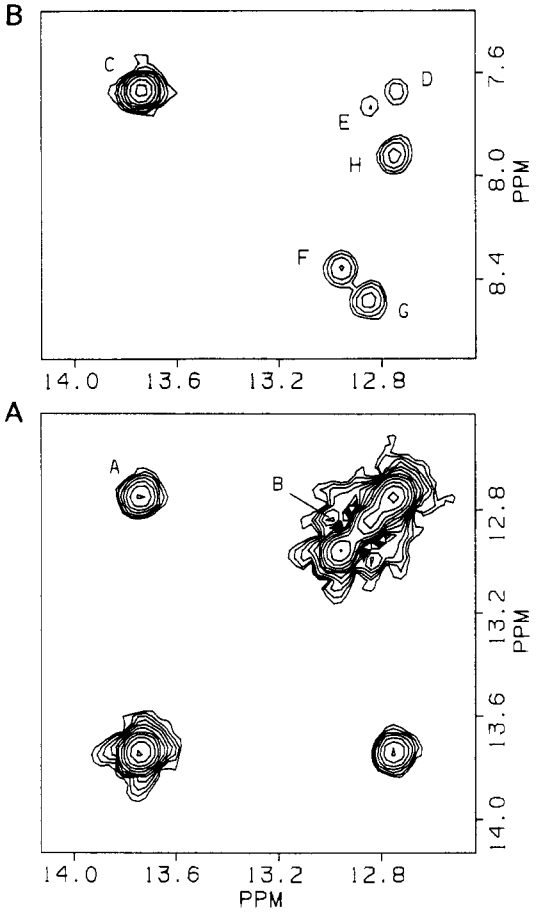

FIGURE 2: Expanded contour plots of the magnitude NOESY spectrum (mixing time 120 ms) of the A·C 12-mer duplex in 1.1 M NaCl, 10 mM phosphate, and H_2O, pH 6.55, at 15 °C. (A) Distance connectivities between imino protons in the symmetrical 12.4–14.0 ppm spectral range. (B) Distance connectivities between the imino protons (12.4–14.0 ppm) and the base and amino protons (7.4–8.8 ppm). The cross-peaks A–H are discussed in the text.

Table I: Exchangeable Proton Chemical Shifts in the A·C 12-mer Duplex at 15 °C[a]

	chemical shifts (ppm)			
base pair	T-H3	G-H1	C-H4[b]	A-H2
G2·C11		12.96	8.37	
C3·G10		12.85	8.49	
A4·C9				7.73
A5·T8	13.74			7.68
G6·C7		12.75	7.93	

[a] Conditions: 1.1 M NaCl, 10 mM phosphate, H_2O, and pH 6.55. [b] Hydrogen-bonded cytidine amino proton.

tidine amino proton (cross-peak G, Figure 2B) within the G·C pair and the 12.96 ppm guanosine imino proton (cross-peak B, Figure 2A) of an adjacent G·C base pair in one direction and the 7.73 ppm adenosine H2 proton (cross-peak E, Figure 2B) of an adjacent A·C base pair in the other direction. This permits assignment of the guanosine imino and cytidine amino protons to the C3·G10 base pair, which is flanked by the G2·C11 and A4·C9 pairs. The remaining 12.96 ppm guanosine imino proton exhibits an NOE to the 8.37 ppm hydrogen-bonded cytidine amino proton (cross-peak F, Figure 2B) and is assigned to the G2·C11 base pair. This completes the assignment of the imino, hydrogen-bonded cytidine amino, and adenosine H2 protons in the A·C 12-mer duplex, pH 6.55, at 15 °C, and these chemical shifts are listed in Table I.

We have undertaken one-dimensional NOE studies on the A·C 12-mer duplex in high-salt H_2O buffer, pH 5.60, 25 °C,

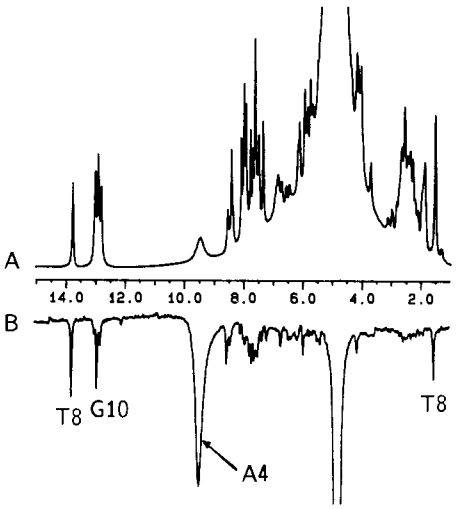

FIGURE 3: (A) The 500-MHz proton NMR spectrum (1–15 ppm) of the A·C 12-mer in 1.1 M NaCl, 10 mM phosphate, and H_2O, pH 5.6, at 25 °C. (B) Difference spectrum following 0.5-s saturation of the 9.38 ppm amino proton of A4. The saturated resonance is designated by an arrow.

in an attempt to assign the exchangeable proton resonance at 9.38 ppm. The control spectrum is plotted in Figure 3A, and the difference spectrum following saturation of exchangeable protons resonating at 9.38 ppm is plotted in Figure 3B. The difference spectrum exhibits NOEs at the imino protons of T8 and G10 and to the CH_3 group of T8, which permits assignment of the protons resonating at 9.38 ppm to the A4·C9 mismatch site which is flanked by C3·G10 and A5·T8 base pairs. Further, this exchangeable proton must be located in the major groove since the thymidine CH_3 group projects into this groove.

The temperature dependence of the A·C 12-mer duplex in high-salt H_2O buffer, pH 6.05, has been recorded between 15 and 45 °C. We note that the 9.38 ppm resonance narrows on raising the temperature and can be readily detected under conditions where the imino protons broaden with increasing temperature. This suggests that the 9.38 ppm resonance corresponds to amino protons at the A4·C9 mismatch site in the A·C 12-mer duplex. The H_2O suppression pulse results in signal attenuation of resonances in the vicinity of the H_2O resonance, and our best intensity estimate relative to that of aromatic and amino proton resonances (7–8.5 ppm) suggests that two protons are responsible for the 9.38 ppm exchangeable resonance in the A·C 12-mer duplex.

Nonexchangeable Proton Spectra. There is a pronounced dependence on pH of the nonexchangeable proton spectrum of the A·C 12-mer in high-salt D_2O buffer. The spectra of the base protons of the A·C 12-mer have been recorded as a function of pH at ambient temperature. These results (Figure 4) demonstrate that raising the pH above 6.5 results in line broadening and changes in chemical shift indicative of structural transitions.

The nonexchangeable base and sugar H1′, H2′, H2″, and H3′ protons in the A·C 12-mer have been assigned by recording a phase-sensitive NOESY spectrum (250-ms mixing time) in high-salt D_2O buffer, pH 6.05 at 25 °C. Contour plots relating the base protons (7.2–8.6 ppm) with the sugar H1′ and cytidine H5 protons (5.2–6.4 ppm) and with the thymidine CH_3 protons (1.5–1.7 ppm) are plotted in panels A and B of Figure 5, respectively. The strongest cross-peaks are observed between the cytidine H6 and H5 protons (interproton separation 2.45 Å), which are designated by asterisks in Figure 5A, and between the thymidine H6 and CH_3 protons

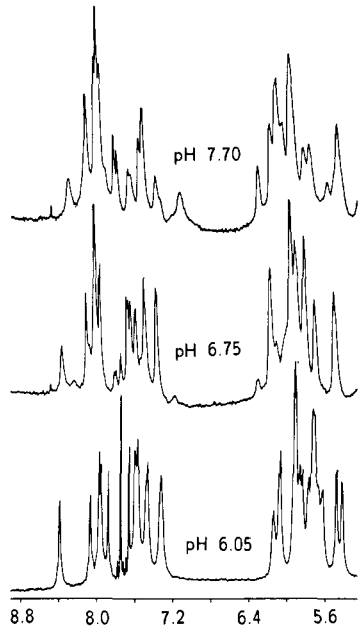

FIGURE 4: The 500-MHz proton NMR spectra (5.4–8.8 ppm) of the A·C 12-mer duplex in 1.1 M NaCl, 10 mM phosphate, and D_2O, 25 °C, at pH 6.05, 6.75, and 7.70.

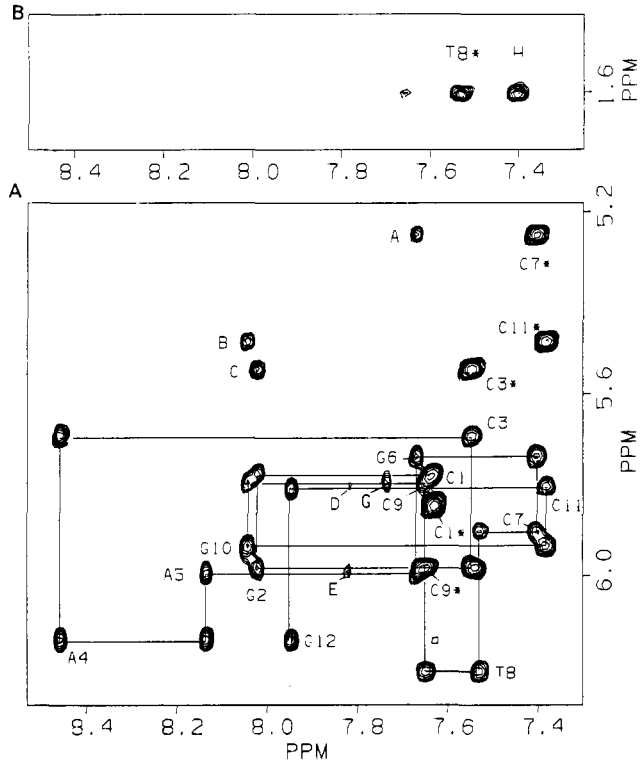

FIGURE 5: Expanded contour plots of the phase-sensitive NOESY spectrum (mixing time 250 ms) of the A·C 12-mer duplex in 1.1 M NaCl, 10 mM phosphate, and D_2O, pH 6.05, at 25 °C. (A) Distance connectivities between the base protons (7.2–8.6 ppm) with the sugar H1′ and cytidine H5 protons (5.2–6.4 ppm). The lines follow connectivities between adjacent base protons through their intervening sugar H1′ protons. (B) Distance connectivities between the base protons (7.2–8.6 ppm) and the thymidine CH_3 protons (1.6–1.7 ppm). The cytidine H6–H5 and the thymidine H6–CH_3 cross-peaks are designated by asterisks. The cross-peaks A–H are discussed in the text.

(interproton separation 3.0 Å), which are designated by asterisks in Figure 5B. All the cross-peaks are well resolved in these expanded contour plots and can be assigned from the directionality of the observed NOE cross-peaks (Hare et al., 1983; Scheek et al., 1984; Weiss et al., 1984). Thus, each base

Table II: Nonexchangeable Proton Chemical Shifts in the A·C 12-mer Duplex at 25 °C[a]

	chemical shifts (ppm)							
base	H8	H2	H6	H5/CH_3	H1′	H2′	H2″	H3′
C1			7.63	5.85	5.78	1.99	2.45	
G2	8.02				5.98	2.74	2.84	5.05
C3			7.55	5.55	5.69	2.25	2.47	4.95
A4	8.46	7.82			6.14	2.72	3.06	5.14
A5	8.13	7.73			5.99	2.64	2.92	5.12
G6	7.67				5.74	2.56	2.64	5.01
C7			7.40	5.25	5.90	2.07	2.55	4.93
T8			7.53	1.61	6.21	2.21	2.63	4.93
C9			7.65	5.98	5.79	1.95	2.36	4.90
G10	8.04				5.93	2.76	2.79	5.07
C11			7.38	5.49	5.80	1.95	2.36	4.86
G12	7.95				6.14	2.44	2.67	

[a] Conditions: 1.1 M NaCl, 10 mM phosphate, D_2O, and pH 6.05.

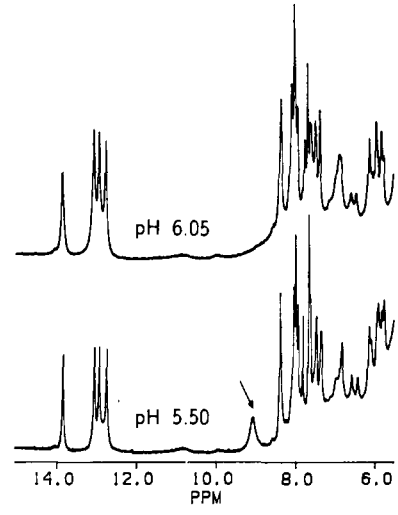

FIGURE 6: The 500-MHz proton NMR spectra (6–15 ppm) of the A·O⁴meT 12-mer duplex in 1.1 M NaCl, 10 mM phosphate, and H_2O, 25 °C, at pH 6.05 and 5.50.

proton (purine H8 or pyrimidine H6) exhibits an NOE to its own and 5′-linked sugar H1′ protons so that it is possible to trace the chain from C1 to G12 as shown in Figure 5A. This tracing is characteristic of right-handed DNA as are the observed cross-peaks for the purine H8(3′–5′)pyrimidine H5/CH_3 dinucleotide steps G2-C3 (cross-peak C, Figure 5A), G6-C7 (cross-peak A, Figure 5A), and G10-C11 (cross-peak B, Figure 5A) and the cross peaks for the pyrimidine H6-(3′–5′)pyrimidine H5/CH_3 dinucleotide step C7-T8 (cross-peak H, Figure 5B). Additional support for a right-handed helix is based on the observed NOEs between the adenosine H2 and nearby sugar H1′ protons. Thus, the H2 of A4 exhibits NOEs to the H1′ protons of A5 on the same strand (cross-peak E, Figure 5A), and the H2 of A5 exhibits NOEs to the H1′ protons of C9 on the partner strand (cross-peak G, Figure 5A). The base and sugar H1′ proton chemical shifts for the A·C 12-mer are listed in Table II. An analysis of the remainder of the NOESY spectrum permits assignment of the H2′, H2″, and H3′ sugar proton chemical shifts, which are also listed in Table II. These sugar proton assignments have been independently checked by recording and assigning through-bond connectivities in a two-dimensional correlated COSY spectrum of the A·C 12-mer duplex.

A·O⁴meT 12-mer

Exchangeable Proton Spectra. The exchangeable proton spectra of the A·O⁴meT 12-mer in high-salt H_2O buffer, at pH 5.5 and pH 6.05, 25 °C, are plotted in Figure 6. Four

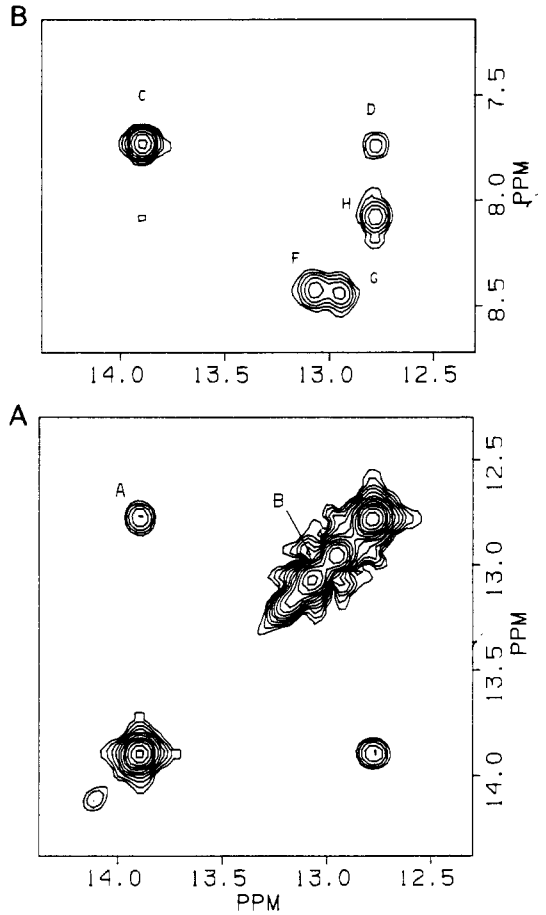

FIGURE 7: Expanded contour plots of the magnitude NOESY spectrum (mixing time 120 ms) of the A·O⁴meT 12-mer duplex in 1.1 M NaCl, 10 mM phosphate, and H_2O, pH 5.9, at 15 °C. (A) Distance connectivities between imino protons in the symmetrical 12.4–14.2 ppm spectral range. (B) Distance connectivities between the imino protons (12.4–14.2 ppm) and the base and amino protons (7.2–8.6 ppm). The cross-peaks A–H are discussed in the text.

imino proton resonances are detected between 12.5 and 14.0 ppm corresponding to three G·C and one A·T nonterminal base pairs. We observe, in addition, an exchangeable proton at 9.04 ppm in the A·O⁴meT 12-mer duplex at 25 °C on lowering the pH to 5.5 (Figure 6).

We have assigned the imino protons in the A·O⁴meT 12-mer in high-salt H_2O buffer, pH 5.9 by recording a magnitude NOESY spectrum (120-ms mixing time) at 15 °C. Contour plots correlating NOEs among imino protons (12.4–14.2 ppm) are plotted in Figure 7A, and those between imino protons (12.4–14.2 ppm) and base and amino protons (7.2–8.6 ppm) are plotted in Figure 7B. The observed cross-peaks are similar to those detected for the A·C 12-mer duplex (Figure 2), and the same procedures are used to make the assignments of the imino protons, the hydrogen-bonded cytidine amino protons, and adenosine H2 protons of the A·O⁴meT 12-mer duplex (Table III). However, one difference between the spectra is that the cross-peak E, which would have corresponded to a NOE between the imino proton of G10 in the C3·G10 base pair and the H2 of A4 in the adjacent A4·O⁴meT9 pair, is either missing or very weak in the A·O⁴meT 12-mer duplex (Figure 7B) while it was observed in the A·C 12-mer duplex (Figure 2B).

We have established the spatial position of the exchangeable resonance at 9.04 ppm in the A·O⁴meT 12-mer duplex from one-dimensional NOE experiments in high-salt H_2O buffer, pH 5.5 at 25 °C (Figure 8). Thus, saturation of the 9.04 ppm resonance results in NOEs at the G10 imino proton of the

Table III: Exchangeable Proton Chemical Shifts in the A·O⁴meT 12-mer Duplex at 15 °C[a]

base pair	chemical shifts (ppm)			
	T-H3	G-H1	C-H4[b]	A-H2
G2·C11		12.97	8.34	
C3·G10		12.86	8.35	
A4·O⁴meT9				7.76
A5·T8	13.81			7.65
G6·C7		12.69	8.00	

[a] Conditions: 1.1 M NaCl, 10 mM phosphate, H_2O, and pH 5.9. [b] Hydrogen-bonded cytidine amino proton.

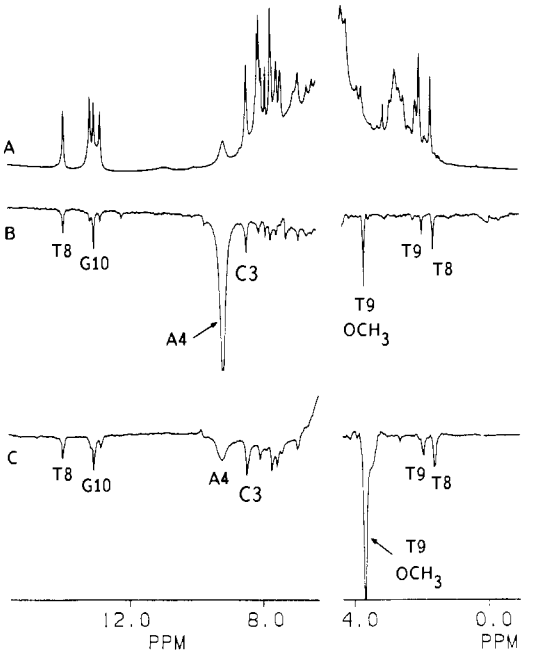

FIGURE 8: (A) The 500-MHz proton NMR spectrum (1–15 ppm) of the A·O⁴meT 12-mer in 1.1 NaCl, 10 mM phosphate, and H_2O, pH 5.5, at 25 °C. (B) Difference spectrum following 0.5-s saturation of the 9.04 ppm amino proton of A4 at 25 °C. (C) Difference spectrum following 0.35-s saturation of the 3.62 ppm OCH_3 resonance of O⁴meT9 at 15 °C. The saturated resonance is designated by an arrow. The difference spectra were corrected with a fourth-order polynomial to flatten the base line.

flanking C3·G10 base pair in one direction and the T8 imino proton of the flanking A5·T8 base pair in the other direction (Figure 8B). More importantly, a NOE is observed to the OCH_3 group of O⁴meT9. The intensity of this NOE is attenuated due to the proximity to the suppressed H_2O resonance. These observations establish that the 9.04 ppm resonance be assigned to the A4·O⁴meT9 modification site and that this exchangeable resonance is located in the major groove. We also note that the NOE observed to the CH_3 group of T8 in the flanking A5·T8 base pair is stronger than that to the CH_3 group of O⁴meT9 in the same A4·O⁴meT9 base pair (Figure 8B). Further, the 3.62 ppm OCH_3 of O⁴meT9 exhibits NOEs to the imino protons of flanking C3·G10 and A5·T8 base pairs and to the amino protons of A4 and a stronger NOE to the CH_3 of adjacent T8 than to the CH_3 of its own O⁴meT9 (Figure 8C). This latter observation was confirmed by parallel studies in D_2O solution. The above results permit us to establish the orientation of the OCH_3 group of O⁴meT9 relative to A4 on the partner strand. We also detect weaker one-dimensional NOEs in the difference spectra recorded in Figure 8B,C, which reflect the contribution of spin diffusion and spillover effects.

The temperature dependence of the A·O⁴meT 12-mer duplex in high-salt H_2O buffer, pH 5.5, has been recorded be-

Table IV: Nonexchangeable Proton Chemical Shifts in the A·O⁴meT 12-mer Duplex at 25 °C[a]

	chemical shifts (ppm)							
base	H8	H2	H6	H5/CH_3	H1′	H2′	H2″	H3′
C1			7.64	5.85	5.78	2.02	2.46	4.72
G2	8.01				5.98	2.70	2.83	5.02
C3			7.49	5.47	5.77	2.25	2.48	4.92
A4	8.40	7.83			6.17	2.66	3.04	5.11
A5	8.06	7.67			5.92	2.56	2.83	5.08
G6	7.71				5.77	2.53	2.64	5.00
C7			7.35	5.17	5.94	2.04	2.51	5.00
T8			7.48	1.58	6.11	2.19	2.62	4.90
O⁴meT9			7.62	1.93	5.95	1.92	2.42	4.90
G10	8.00				5.85	2.67	2.73	5.02
C11			7.38	5.42	5.84	1.92	2.36	4.82
G12	7.93				6.13	2.39	2.64	4.70

[a] Conditions: 1.1 M NaCl, 10 mM phosphate, D_2O, and pH 5.5.

tween 10 and 35 °C. The 9.04 ppm resonance exhibits a shoulder on lowering the temperature to 10 °C. The 9.04 ppm exchangeable resonance exhibits an area of ~2 protons relative to that of the aromatic and amino proton resonances (7–8.5 ppm) in the A·O⁴meT 12-mer duplex.

Nonexchangeable Proton Spectra. There is a pronounced pH dependence in the nonexchangeable proton spectra of the A·O⁴meT 12-mer duplex similar to that observed for the A·C 12-mer duplex. The base proton spectrum of the A·O⁴meT 12-mer duplex have been recorded as a function of pH in Figure 9. The narrow resonances in the low-pH spectrum broaden on raising the pH, and there are chemical shift changes indicative of structural transitions.

Phase-sensitive NOESY spectra (mixing time 250 ms) of the A·O⁴meT 12-mer duplex have been recorded in high-salt D_2O buffer, 25 °C at pH 5.5. Regions of the pH 5.5 data set correlating the base protons (7.3–8.5 ppm) with the sugar H1′ and cytidine H5 protons (5.2–6.2 ppm) and with the CH_3 protons (1.5–1.9 ppm) are plotted in panels A and B of Figure 10, respectively. The purine H8 and pyrimidine H6 base protons can be readily traced from C1 to G12 by stepping through the sugar H1′ protons as shown in Figure 10A. The observed cross-peaks between protons of adjacent bases in purine(3′–5′)pyrimidine steps (cross-peaks A–C, Figure 10A), between protons of adjacent bases in pyrimidine(3′–5′)pyrimidine steps (cross-peaks H and I, Figure 10B), and between adenosine H2 and flanking sugar H1′ protons (cross-peaks E and G, Figure 10A) demonstrate that the duplex is right-handed. We have also analyzed the distance connectivities in other regions of the NOESY plots as well as through-bond COSY plots, to assign the chemical shifts of the base protons and sugar H1′, H2′, H2″, and H3′ protons of the A·O⁴meT 12-mer duplex at 25 °C (Table IV).

We have recorded one-dimensional slices through the H6 and CH_3 protons of O⁴meT9 and have not detected measurable NOEs to the OCH_3 group in the NOESY spectrum of the A·O⁴meT 12-mer duplex. This provides additional evidence that the OCH_3 group at position 4 is directed away from the CH_3 group at position 5 on the O⁴meT base.

Discussion

The present two-dimensional NMR study has focused on the pairing properties of the A·O⁴meT lesion located four base pairs in from either end of the self-complementary dodecanucleotide duplex (II), and these results are compared with the corresponding A·C mismatch located at the same position in the sequence (I). The current two-dimensional NMR studies on the A·C mismatch expand on previous one-dimensional NMR studies (Patel et al., 1984a,b), which proposed wobble A·C base pair formation when the mismatch was located three base pairs in from either end of self-complementary dodecanucleotide duplex in aqueous solution.

Conformational Transitions. The base and sugar H1′ proton spectra of the A·C 12-mer in high-salt D_2O buffer between pH 6.05 and pH 7.70 (Figure 4) clearly demonstrate a pH-dependent change in conformation. The predominant conformation at pH 6.05 exhibits narrower proton spectra compared to the conformation(s) that predominate at pH 7 and above (Figure 4). A similar pH-dependent structural change is seen in the A·O⁴meT 12-mer duplex in high-salt D_2O buffer between pH 5.5 and pH 7.35 (Figure 9). Once again the structure that predominates at pH 5.5 has narrower resonances than the structure(s) that predominate(s) at higher pH values. Our efforts have therefore focused on the conformation of the A·C 12-mer duplex and the A·O⁴meT 12-mer duplex in the pH 5.5–6.0 range where high-quality two-dimensional NOESY data sets can be collected from the nonexchangeable protons.

Imino Proton Spectra. The imino proton spectra (12.5–14.0 ppm) in the A·C 12-mer duplex (Figure 1) and the A·O⁴meT 12-mer duplex (Figure 6) were similar with the four resolved resonances corresponding to the imino protons from the nonterminal Watson–Crick G2·C11, C3·G10, A5·T8, and G6·C7 base pairs. These resonances have been assigned to specific imino protons from NOESY studies on the A·C 12-mer duplex in high-salt H_2O buffer at 15 °C (Figure 2) and the A·O⁴meT 12-mer duplex in high-salt H_2O buffer at 15 °C (Figure 7). These studies demonstrate intact C3·G10 and A5·T8 base pairs on either side of the modification site in the A·C 12-mer and A·O⁴meT 12-mer duplexes.

Amino Proton Spectra. A novel feature of our studies is the observation of an exchangeable resonance at 9.38 ppm in the spectra of the A·C 12-mer duplex at pH 6.05 at 25 °C (Figure 1) and at 9.04 ppm in the spectra of the A·O⁴meT 12-mer duplex at pH 5.5 at 25 °C (Figure 6). We assign this resonance to the amino protons of A in the A·C 12-mer and A·O⁴meT 12-mer for the following reasons: First, this resonance exhibits an area of approximately two protons when compared with the area of exchangeable and nonexchangeable protons in the 7–8.5 ppm region. Second, the Watson–Crick imino protons between 12.5 and 14.0 ppm are far more labile to exchange than this ~9.2 ppm exchangeable resonance in the A·C 12-mer duplex and the A·O⁴meT 12-mer duplex, consistent with assignment of the ~9.2 ppm exchangeable resonance to amino rather than imino protons. Third, the NOEs between these amino protons and the imino protons of the flanking C3·G10 and A5·T8 base pairs for both the A·C 12-mer duplex (Figure 3) and the A·O⁴meT 12-mer duplex (Figure 8) establish that the ~9.2 ppm resonance corresponds to the same protons in the A·C mismatch pair and the A·O⁴meT pair. This limits the assignment to the amino protons of A4, which are common to the A4·C9 mismatch and the A4·O⁴meT9 pair. The amino protons of A4 are located in the major groove and exhibit NOEs to the CH_3 protons of adjacent T8 located in the major groove on the partner strand in the A·C 12-mer duplex (Figure 3) and the A·O⁴meT 12-mer duplex (Figure 8). We note, however, that the observation of average narrow resonances at ~9.2 ppm for the amino protons of A in the A·C 12-mer (Figure 1) and A·O⁴meT 12-mer (Figure 6) duplexes at low pH contrasts with our expectation of separate resonances for the hydrogen-bonded and exposed protons (Patel, 1976; McConnel, 1984; Boelens et al., 1985).

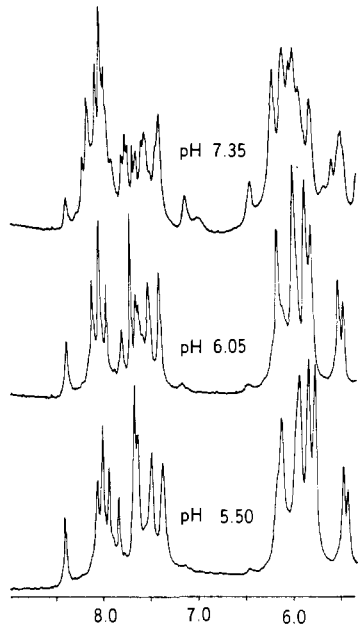

FIGURE 9: The 500-MHz proton NMR spectra (5.4–8.6 ppm) of the A·O⁴meT 12-mer duplex in 1.1 M NaCl, 10 mM phosphate, and D_2O, 25 °C, at pH 5.5, 6.05, and 7.35.

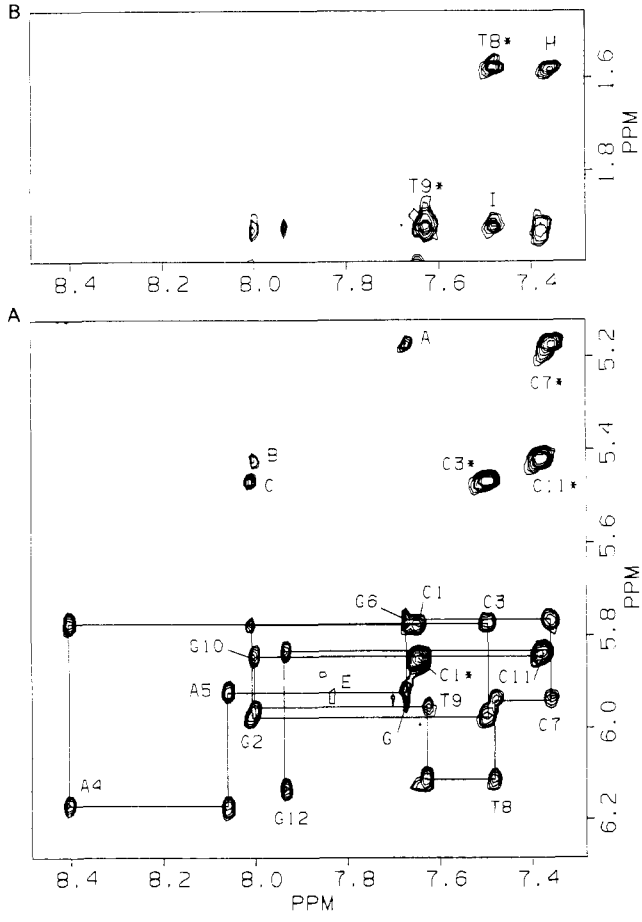

FIGURE 10: Expanded contour plots of the phase-sensitive NOESY spectrum (mixing time 250 ms) of the A·O⁴meT 12-mer duplex in 1.1 M NaCl, 10 mM phosphate, and D_2O, pH 5.5, at 25 °C. Distance connectivities between the base protons (7.3–8.5 ppm) with the sugar H1′ and cytidine H5 protons (5.2–6.2 ppm) and with the CH_3 protons (1.6–1.8 ppm) are plotted in (A) and (B), respectively.

A major conclusion of the present study is the demonstration that the detection of the amino protons of A4 is linked to the formation of the low-pH conformation of the A·C 12-mer and A·O⁴meT 12-mer duplexes.

Table V: Nonexchangeable Proton Chemical Shifts in the A·T 12-mer Duplex and Chemical Shift Changes on Proceeding from the A·T 12-mer Duplex to the A·C 12-mer and A·O⁴meT 12-mer Duplexes[a]

	chemical shifts (ppm)		
	A·T 12-mer	A·C 12-mer	A·O⁴meT 12-mer
C3·G10			
G-H8	7.96	0.08	0.04
C-H6	7.39	0.16	0.10
C-H5	5.49	0.06	−0.02
G-H1′	5.87	0.06	−0.02
C-H1′	5.48	0.21	0.29
A4·O⁴meT9/C9			
A-H8	8.26	0.20	0.14
A-H2	7.36	0.46	0.47
T-H6/C-H6	7.38	0.27	0.24
T-CH_3	1.73		0.20
A-H1′	5.84	0.30	0.33
T-H1′/C-H1′	5.86		0.09
A5·T8			
A-H8	8.11	0.02	−0.05
A-H2	7.55	0.18	0.12
T-H6	7.49	0.04	−0.01
T-CH_3	1.60	0.01	−0.02
A-H1′	6.02	−0.03	−0.10
T-H1′	6.11	0.10	0.00

[a] Conditions: 1.1 M NaCl, 10 mM phosphate, and D_2O. The pH of the A·T 12-mer duplex was 6.4, the pH of the A·C 12-mer duplex was 6.05, and the pH of the A·O⁴meT 12-mer duplex was 5.5.

Nonexchangeable Protons. We detect striking similarities in the NOE connectivities between the base protons (7.2–8.6 ppm) and the sugar H1′ and cytidine H5 protons (5.2–6.4 ppm) in the A·C 12-mer duplex, pH 6.05, 25 °C (Figure 5), and the A·O⁴meT 12-mer duplex, pH 5.5, 25 °C (Figure 10). Further, the A4 and C9 base protons exhibit NOEs to their own and 5′-flanking sugar H1′ protons in the A·C 12-mer duplex (Figure 5A) as do the A4 and O⁴meT9 residues in the A·O⁴meT 12-mer duplex (Figure 10A). This establishes that the A·C 12-mer duplex is right-handed and that A4 and C9 are stacked into the helix. Similarly, the A·O⁴meT 12-mer duplex is right-handed with A4 and O⁴meT9 also stacked into the helix. Further, the H8 of A4 has similar downfield shifts in the A·C 12-mer duplex, pH 6.05 (8.45 ppm, Figure 5A), and the A·O⁴meT 12-mer duplex, pH 5.5 (8.4 ppm, Figure 10A).

The chemical shift of the H8 proton of A4 provides a useful marker for monitoring the pH-dependent conformational transition in the A·C 12-mer duplex (Figure 4) and the A·O⁴meT 12-mer duplex (Figure 9). This proton exhibits a downfield shift of ~0.1 ppm associated with the conversion from high- to low-pH conformations of both these duplexes. Interestingly, the pH-independent chemical shift of the H8 proton of A4 in the control A·T 12-mer duplex (8.26 ppm at 25 °C) exhibits the same value as that detected for the high-pH conformations of the A·C 12-mer and A·O⁴meT 12-mer duplexes.

We note that the exchangeable and nonexchangeable protons in the A·C 12-mer duplex (Tables I and II) and the A·O⁴meT 12-mer duplex (Tables III and IV) have very similar chemical shifts. The largest difference is 0.16 ppm between the H1′ proton of C9 in the A·C 12-mer and O⁴meT9 in the A·O⁴meT 12-mer (Tables II and IV). These results also indicate a similar conformation at the A·C and A·O⁴meT modification site.

We have also recorded and analyzed the NOESY spectra of the control A·T 12-mer duplex in H_2O and D_2O solution.

It is instructive to compare the chemical shift differences for the A·C 12-mer and A·O⁴meT 12-mer duplexes relative to the control A·T 12-mer duplex both at the modified base pair and its flanking pairs. These results are summarized in Table V and include the chemical shifts of the nonexchangeable protons of C3·G10, A4·T9, and A5·T8 base pairs in the A·T 12-mer duplex and the chemical shift differences with the corresponding resonances for the A·C 12-mer duplex and the A·O⁴meT 12-mer duplex. We observe a large downfield shift (~0.46 ppm) at the H2 proton of A4 and a smaller downfield shift (~0.15 ppm) of the H2 proton of A5 on replacement of the A·T Watson–Crick base pair by either the A·C mismatch pair or the A·O⁴meT pair (Table V). These downfield shifts are consistent with the sliding of the A4 base into the minor groove on formation of wobble pairs resulting in a reduced overlap of the H2 proton of A4 with adjacent base pairs. Further, downfield shifts are also detected at the sugar H1′ protons of C3 (~0.25 ppm) and A4 (~0.31 ppm) (Table V), suggestive of small glycosidic torsion angle changes at these positions when A·C and A·O⁴meT pairs replace the A·T pair.

Structure of A·C Mismatch Pair and A·O⁴meT Pair. The current model of A·C mismatch pair structure based on one-dimensional NMR studies (Patel et al., 1984a,b), theoretical computations guided by NMR measurements (Keepers et al., 1984), and single-crystal X-ray studies at atomic resolution (Hunter et al., 1986) is

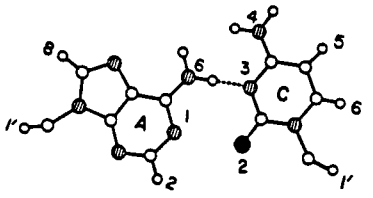

III

The A and C residues form a wobble pair with a hydrogen bond between the 6-amino group of A and the N3 of C. The ring N1 of A and the carbonyl O2 of C are positioned to form a second hydrogen bond through ring protonation. The possibility of such a protonation has been previously considered on the basis of the downfield proton chemical shift of the H8 of A at the A·C mismatch site in the dodecanucleotide studied previously [Patel et al., 1984; see also Sowers et al. (1986)] and from the short adenosine N1 to cytidine O2 separation for the A·C mismatch in a dodecanucleotide crystal (Hunter et al., 1986).

There remain unanswered questions at this stage concerning formation of protonated A·C pairs for the low-pH structure of the A·C 12-mer duplex and protonated A·O⁴meT pairs for the low-pH structure of the A·O⁴meT 12-mer duplex. We have not detected a resonance that could be assigned to a proton between the N1 atom of A and the O2 atom of C/O⁴meT. Possibly, this could reflect its high rate of exchange. The resolution of this question must await NMR studies on the same sequences with ^{15}N labels incorporated at the N1 and N6 of A and the N3 of C/O⁴meT (^{15}N resonances shift ~80 ppm on protonation).

The striking similarity between the exchangeable and nonexchangeable proton spectra along with the NOESY cross-peak patterns for the A·C 12-mer and A·O⁴meT 12-mer duplexes suggest that the wobble base pair structure for the A·C mismatch (III) can be extended to the A·O⁴meT lesion (IV):

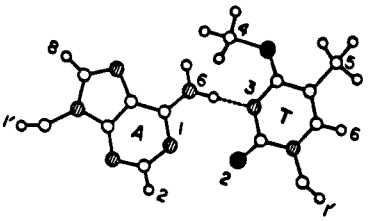

IV

Single-crystal X-ray studies for O⁴-methyluridine (Brennan et al., 1983), O⁴-methylthymidine (Brennan et al., 1986), and O⁴-ethylthymidine (Birnbaum et al., 1986) show that in each case the *O*-alkyl group adopts a periplanar conformation syn to N3. We have distinguished between syn and anti orientations of the OCH_3 group of O⁴meT9 from the relative magnitude of the observed NOEs to other nearby protons. The NOE detected between the 9.04 ppm amino proton of A4 and the OCH_3 group of O⁴meT9 (Figure 8B) establishes that the OCH_3 group is syn and directed toward the A4 residue on the partner strand. Strong support for this syn orientation is based on the observation of a much stronger NOE from the OCH_3 group of O⁴meT9 to the CH_3 group of flanking T8 compared to the CH_3 of its own O⁴meT9.

Registry No. A·C 12-mer, 111616-40-1; A·O⁴meT 12-mer, 106251-76-7; adenine, 73-24-5; cytosine, 71-30-7; *O*⁴-methylthymine, 25902-89-0.

REFERENCES

Birnbaum, G. I., Sadana, K. L., Blonski, W. J., & Hruska, F. E. (1986) *J. Am. Chem. Soc. 108*, 1671–1675.

Boelens, R., Scheek, R. M., Dijkstra, K., & Kaptein, R. (1985) *J. Magn. Reson. 62*, 378–386.

Brennan, R. G., Prive, G. G., Blonski, W. J., Hruska, F. E., & Sundaralingam, M. (1983) *J. Am. Chem. Soc. 105*, 7737–7742.

Brennan, R. G., Pyzalska, D., Blonski, W. J., Hruska, F. E., & Sundaralingam, M. (1986) *Biochemistry 25*, 1181–1185.

Hare, D. R., Wemmer, D. E., Chou, S. H., Drobny, G. & Reid, B. R. (1983) *J. Mol. Biol. 171*, 319–336.

Hunter, W. N., Brown, T., Anand, N. N., & Kennard, O. (1986) *Nature (London) 320*, 552–555.

Kalnik, M. W., Kouchakdjian, M., Li, B. F. L., Swann, P. F., & Patel, D. J. (1988) *Biochemistry* (following paper in this issue).

Keepers, J. W., Schmidt, P., James, T. L., & Kollman, P. A. (1984) *Biopolymers 23*, 2901–2929.

Klevitt, R. E. (1985) *J. Magn. Reson. 62*, 551–555.

Li, B. F., Reese, C. B., & Swann, P. F. (1987) *Biochemistry 26*, 1086–1093.

McConnel, B. (1984) *J. Biomol. Struct. Dyn. 1*, 1407.

Otting, G., Widmer, H., Wagner, G., & Wuthrich, K. (1986) *J. Magn. Reson. 66*, 187–193.

Patel, D. J. (1976) *Biopolymers 15*, 533–558.

Patel, D. J., Kozlowski, S. A., Ikuta, S., & Itakura, K. (1984a) *Biochemistry 23*, 3218–3226.

Patel, D. J., Kozlowski, S. A., Ikuta, S., & Itakura, K. (1984b) *Fed. Proc., Fed. Am. Soc. Exp. Biol. 43*, 2663–2670.

Pegg, A. E. (1977) *Adv. Cancer Res. 25*, 195–267.

Preston, B. D., Singer, B., & Loeb, L. A. (1986) *Proc. Natl. Acad. Sci. U.S.A. 83*, 8501–8505.

Scheek, R. M., Boelens, R., Russo, N., van Boom, J. H., & Kaptein, R. (1984) *Biochemistry 23*, 1371-1376.
Singer, B., & Grunberger, D. (1983) in *Molecular Biology of Mutagens and Carcinogens*, Plenum, New York.
Sowers, L. C., Fazakerley, G. V., Kim, H., Dalton, L., & Goodman, M. F. (1986) *Biochemistry 25*, 3983-3988.
Weiss, M. A., Patel, D. J., Sauer, R. T., & Karplus, M. (1984) *Proc. Natl. Acad. Sci. U.S.A. 81*, 130-134.

Base Pair Mismatches and Carcinogen-Modified Bases in DNA: An NMR Study of G·T and G·O^{4}meT Pairing in Dodecanucleotide Duplexes†

Matthew W. Kalnik,‡ Michael Kouchakdjian,‡ Benjamin F. L. Li,§,‖ Peter F. Swann,§ and Dinshaw J. Patel*,‡

Department of Biochemistry and Molecular Biophysics, College of Physicians and Surgeons, Columbia University, New York, New York 10032, and Courtauld Institute of Biochemistry, Middlesex Hospital Medical School, London, England W1P 7PN

Received June 23, 1987; Revised Manuscript Received September 8, 1987

ABSTRACT: High-resolution two-dimensional NMR studies have been completed on the self-complementary d(C-G-C-*G*-A-G-C-T-*T*-G-C-G) duplex (designated G·T 12-mer) and the self-complementary d(C-G-C-*G*-A-G-C-T-*O^{4}meT*-G-C-G) duplex (designated G·O^{4}meT 12-mer) containing G·T and G·O^{4}meT pairs at identical positions four base pairs in from either end of the duplex. The exchangeable and nonexchangeable proton resonances have been assigned from an analysis of two-dimensional nuclear Overhauser enhancement (NOESY) spectra for the G·T 12-mer and G·O^{4}meT 12-mer duplexes in H_2O and D_2O solution. The guanosine and thymidine imino protons in the G·T mismatch resonate at 10.57 and 11.98 ppm, respectively, and exhibit a strong NOE between themselves and to imino protons of flanking base pairs in the G·T 12-mer duplex. These results are consistent with wobble pairing at the G·T mismatch site involving two imino proton–carbonyl hydrogen bonds as reported previously [Hare, D. R., Shapiro, L., & Patel, D. J. (1986) *Biochemistry 25*, 7445-7456]. In contrast, the guanosine imino proton in the G·O^{4}meT pair resonates at 8.67 ppm. The large upfield chemical shift of this proton relative to that of the imino proton resonance of G in the G·T mismatch or in G·C base pairs indicates that hydrogen bonding to O^{4}meT is either very weak or absent. This guanosine imino proton has an NOE to the OCH_3 group of O^{4}meT across the pair and NOEs to the imino protons of flanking base pairs. Taken together with data from the NMR of nonexchangeable protons, this shows that both G and O^{4}meT have anti-glycosidic torsion angles and are stacked into the duplex. Comparison of the intensity of the NOEs between the guanosine imino proton and the OCH_3 of O^{4}meT as well as other protons in its vicinity demonstrates that the OCH_3 group of O^{4}meT adopts the syn orientation with respect to N3 of the methylated thymidine. This rules out both the wobble pairing and the postulated structure in which the imino proton of G is hydrogen bonded to N3 of O^{4}meT for the G·O^{4}meT pair. We propose an alternate base pairing mode stabilized by one short hydrogen bond between the 2-amino group of guanosine and the 2-carbonyl group of O^{4}meT.

The base pairing properties of O^4-methylthymidine (O^{4}meT) are of considerable interest because of the importance of this alkylated base in the carcinogenic and mutagenic action of *N*-nitroso compounds (Swenberg et al., 1984; Singer, 1986). It is widely believed that *O*^{4}-alkylthymidine forms a base pair with guanosine in DNA because *O*^{4}-alkylthymidine is incorporated into DNA by DNA polymerase only in the presence of templates containing guanosine bases (Hall & Saffhill, 1983) and guanosine is incorporated when oligonucleotides containing O^{4}meT are used as templates for DNA synthesis (Singer et al., 1986). Further, the presence of O^{4}meT residues in the DNA of ϕX-174 phage results in A·T → G·C transitions at the original alkylation site (Preston et al., 1986). Hypothetical structures for this pair have been proposed (Brennan et al., 1986), but there is no structural information at the molecular level on the pairing properties of the alkylated base. This has led us to systematically study the NMR properties of the G·O^{4}meT pair in oligonucleotide duplexes and compare the spectral parameters with those for the G·T mismatch pair in otherwise identical duplexes. This paper focuses on a comparative study of self-complementary dodecanucleotides of the general sequence d(C-G-C-*X*-A-G-C-T-*Y*-G-C-G), which after annealing form a duplex containing internal G·T mismatches (X = G and Y = T) and G·O^{4}meT base pairs (X = G and Y = O^{4}meT).

The G·T mismatch, first studied with poly d(G-T) by NMR (Early et al., 1978), has been characterized in detail by one-dimensional NMR (Patel et al., 1982) and by two-dimensional NMR–distance geometry studies on solutions of oligodeoxydodecanucleotides (Hare et al., 1986), as well as by theoretical computation (Chuprina & Poltev, 1983; Keepers et al., 1984) and single-crystal X-ray diffraction (Kneale et al., 1985).

† The research was supported from Start-Up Funds provided by Columbia University, by NIH Grant CA-46533 to D.J.P., and by grants from the Cancer Research Campaign and the Medical Research Council to P.F.S. The NMR spectrometers were purchased from funds donated from the Robert Woods Johnson Jr. Trust and Matheson Trust toward setting up an NMR Center in the Basic Medical Sciences at Columbia University.

‡ Columbia University.
§ Middlesex Hospital Medical School.
‖ Present address: Institute of Molecular and Cellular Biology, National University of Singapore, Kent Ridge, Singapore 0511.

0006-2960/88/0427-0108$01.50/0